Math. Model. Nat. Phenom.
Vol. 7, No. 1, 2012, pp. 306-336
DOI: 10.1051/mmnp/20127114

Modeling the Impact of Anticancer Agents on Metastatic Spreading

S. Benzekry[1,2], N. André[3,4], A. Benabdallah[1], J. Ciccolini[2] C. Faivre[2], F. Hubert[1] and D. Barbolosi[2] *

[1] CMI-LATP, UMR 6632, Université de Provence, Technopôle Château-Gombert
39, rue F. Joliot-Curie, 13453 Marseille cedex 13, France
[2] Laboratoire de Toxicocinétique et Pharmacocinétique UMR INSERM 911, CRO2
27, boulevard Jean Moulin, 13005 Marseille, France
[3] Service d'Hématologie et Oncologie Pédiatrique, Hôpital pour enfants de La Timone
Marseille, France
[4] Metronomics Global Health Initiative

Abstract. Treating cancer patients with metastatic disease remains an ultimate challenge in clinical oncology. Because invasive cancer precludes or limits the use of surgery, metastatic setting is often associated with (poor) survival, rather than sustained remission, in patients with common cancers like lung, digestive or breast carcinomas. Mathematical modeling may help us better identify non detectable metastatic status to in turn optimize treatment for patients with metastatic disease. In this paper we present a family of models for the metastatic growth. They are based on four principles : to be as simple as possible, involving the least possible number of parameters, the main informations are obtained from the primary tumor and being able to recover the variety of phenomena observed by the clinicians. Several simulations of therapeutic strategies are presented illustrating possible applications of modeling to the clinic.

Key words: modeling, metastases, anti-angiogenic therapy, metronomic chemotherapy
AMS subject classification: 35F16, 92C50

*Corresponding author. E-mail: fhubert@cmi.univ-mrs.fr

Article published by EDP Sciences and available at http://www.mmnp-journal.org or http://dx.doi.org/10.1051/mmnp/20127114
https://doi.org/10.1051/mmnp/20127114 Published online by Cambridge University Press

1. Introduction

Classification of cancer as localized or metastatic disease remains the mainstay for determining the best therapeutic strategy to be undertaken at bedside. Although simple, this classification may underestimate the risk of undetectable, early metastatic stages [17]. Many studies have been performed to identify prognostic biomarkers for evaluating the risk of metastatic relapse in patients with apparently localized disease. We have developed original mathematical models designed to evaluate the metastatic state of the patient. These models including the efficacy of some anticancerous drugs, are designed to help clinicians to define the best therapeutic strategy.

Our approach consists in deriving a transport equation for the metastatic colony distribution ranged by some physiological traits denoted by $X \in \mathbb{R}^n$ of the tumor growth, for example $X = x$ the size of the tumor (= Volume, either expressed in number of cells or mm^3, using the conversion rule 1 mm$^3 \simeq 10^6$ cells). We suppose that the primary tumor is generated by a single cell at $t = 0$ and grows with the rate $G(t, X)$ per time unit. The growing tumor emits metastatic cells with the rate $\beta(X)$. Each metastatic cell develops into a new tumor, which also grows at rate $G(t, X)$ and emits new nuclei of metastasis just as the primary tumor does. Let $\rho(t, X)$ represent the colony distribution structured by the trait X at time t. The dynamics of the colony distribution is then given by the following Mac-Kendrick Von Foerster equation:

$$\begin{cases} \frac{\partial}{\partial t}\rho(t,X) + \mathrm{div}[G(t,X)\rho(t,X)] = 0, & X \in \Omega,\ t \geq 0 \\ -G(t,\sigma)\cdot\nu\rho(t,\sigma) = N(\sigma)\left\{\int_\Omega \beta(X)\rho(t,X)dX\ +\ \beta(X_p(t))\right\}, & \sigma \in \partial\Omega,\ t \geq 0 \\ \rho(0,X) = 0, & X \in \Omega \end{cases} \tag{1.1}$$

with $X_p(t)$, representing evolution of the primary tumor in the trait space satisfies $\dot{X}_p(t) = G(t, X_p(t))$ and N is the distribution of metastases at birth. From the solution ρ of this partial differential equation problem, various quantities of interest can be derived :

$$\text{Total number of metastases} = \int_\Omega \rho(t,X)dX, \quad \text{Visible metastases} = \int_\Omega \mathbf{1}_{x\geq x_{vis}}(X)\rho(t,X)dX$$

$$\text{Metastatic mass} = \int_\Omega x\rho(t,X)dX$$

with x_{vis} being the threshold for metastases to be visible (typically, 10^7 cells).

The first model in that direction was derived in [28] where the tumor growth follows some Gompertz law. The variable $X \in \mathbb{R}$ is the size of the tumor and for untreated tumor $G(t, X) = aX\ln(\theta/X)$. The potentialities of this model have been widely discussed in [2, 18, 45, 5]. The section 2 is devoted to introduction of a chemotherapy in this previous model. We exhibit how the model can give some hints on the choice of the number of cycles for a cytotoxic drug in a post-surgery context (adjuvant chemotherapy). Because most anticancer drugs are highly toxic, tolerance is an issue because treatment has often to be discontinued in patients with severe toxicities (eg, hematologic). In addition to standard cytotoxic agents all displaying a poor efficacy/toxicity balance, targeted therapies (eg, anti-angiogenic drugs as monoclonal antibodies or tyrosin kinase inhibitors) have emerged as a new paradigm to treat patients with cancer in a safer manner.

https://doi.org/10.1051/mmnp/20127114 Published online by Cambridge University Press

In the section 3. we explain how to integrate the action of these drugs within our approach. In this model, developed in [7, 8, 9], the tumor growth rate is bi-dimensional and integrates dynamics of the vascular capacity following the model of [26]. We first study and compare effect of the scheduling of anti-angiogenic drugs on both primary tumor growth and metastases. Then, we propose a model to take into account the metastatic acceleration phenomenon reported in [20] after Sunitinib therapy.

Metronomic chemotherapy [38] - the chronic administration of chemotherapy at relatively low, minimally toxic doses on a frequent schedule of administration, at close regular intervals, with no prolonged drug-free breaks - have been recently developed to reduce the toxic-risk in patients. This novel approach is an alternative way for fragile patients as children and old patients [1, 6, 14, 43, 16, 32, 44, 22]. These therapies seem to exhibit an anti-angiogenic effect on the tumor [31, 25] and reveal to be more efficient than classical cytotoxic therapies on large times. For such new therapeutical strategies, modeling should be of great help to give some prediction of the efficacy of the treatment. In section 5., we propose a model for such therapies. Numerical experiments reinforce constations of the clinicians, that is long time gain of metronomic chemotherapy.

2. Adjuvant chemotherapy

2.1. Model

We assume here that the tumor growth follows some Gompertz law with parameter a (proliferation rate, related to the tumor doubling time, taken constant) and $\theta > 1$ (carrying capacity = maximum tumor size). The chemotherapy treatment (CT) then acts as a reduction of the growth speed *via* a log-kill term, that is

$$G(t,x) = ax \ln\left(\frac{\theta}{x}\right) - C(t)(x - x_{min})^+ \tag{2.1}$$

where $t \mapsto C(t)$ stands for the exposure of the cancer cells to the drug which is given by the pharmacokinetics (PK)/pharmacodynamics (PD) model, and x_{min} is the minimal size for the treatment to be active (size of one cell). The PK model for Docetaxel is a three-compartmental model, coming from [13]. We use the interface model from [36] as PD model. All together, the equations are

$$\begin{cases} \dot{c}_1(t) = -k_e c_1(t) + k_{12}(c_1(t) - c_2(t)) - k_{13}(c_1(t) - c_3(t)) + \frac{I(t)}{V} \\ \dot{c}_2(t) = k_{21}(c_1(t) - c_2(t)) \\ \dot{c}_3(t) = k_{31}(c_1(t) - c_3(t)) \\ \dot{C}(t) = -\alpha_I e^{-\beta_I C(t)} C(t) + c_1(t) \end{cases} \tag{2.2}$$

The last equation is the interface model introduced in [36] to model the effect (exposure) $C(t)$ of the drug, the variables c_1, c_2, c_3 denote the concentrations in the three compartments and V some specific volume associated to the first compartment. It is intended to have more flexibility than just considering the area under the curve (which is obtained by taking $\alpha_I = 0$) or an effect

https://doi.org/10.1051/mmnp/20127114 Published online by Cambridge University Press

compartment ($\beta_I = 0$). The term I stands for the drug input and writes

$$I(t) = \sum_{i=1}^{M} D_i \mathbf{1}_{t_i \leq t \leq t_i + \tau} \tag{2.3}$$

where $\{t_i;\ i = 1, .., M\}$ are the administration times of the drug, $\{D_i;\ i = 1, .., M\}$ the administrated doses and τ the injection duration. The parameter values used for the PK model can be found in Table 1.

Parameter	V	k_{12}	k_{13}	k_e	k_{21}	k_{31}
Value	7.4	25.44	30.24	123.8	36.24	2.016
Unit	L	day^{-1}	day^{-1}	day^{-1}	day^{-1}	day^{-1}

Table 1: Parameter values of the PK model for Docetaxel [13].

The density of metastases $\rho(t, x)$ structured in size x of the tumor as in [28, 2] solves:

$$\frac{\partial}{\partial t}\rho(t,x) + \frac{\partial}{\partial x}[G(t,x)\rho(t,x)] = 0,\ x \in [1, \theta),\ t \geq 0 \tag{2.4-a}$$

$$g(1)\rho(1,t) = \int_1^b \beta(x)\rho(x,t)dx\ +\ \beta(x_p(t)), \tag{2.4-b}$$

$$\rho(x,0) = 0. \tag{2.4-c}$$

where

1. Equation (2.4-b) relates the creation of metastases.
2. The number of cells $x_p(t)$ in the primary tumor at time t is the solution of the ordinary differential equation the Cauchy problem: $\frac{d}{dt}x_p(t) = G(t, x_p(t)),\ x_p(0) = 1$.
3. The colonization rate $\beta(x)$ is choosen as:

$$\beta(x) = mx^{\alpha}, \tag{2.5}$$

where m is the colonization coefficient and α is the fractal dimension of blood vessels infiltrating the tumor. The parameter α expresses how blood vessels geometrically distribute in or on a tumor. If vasculature is superficial the fractal dimension α is assigned to be $2/3$ because assuming that the tumor has the shape of a sphere implies that the surface area is proportional to $2/3$. Otherwise, in the case of an homogeneously distributed vasculature in the whole tumor, α is taken to be equal to 1.

Note that for each patient, we have to identify the parameters involved in the model. A calibration of the model for non treated tumors has been done in [5] thanks to a clinical study performed in Institut Gustave Roussy between 1958 and 1972 (see [33]).

https://doi.org/10.1051/mmnp/20127114 Published online by Cambridge University Press

2.2. Some features on adjuvant chemotherapy

The following section illustrates how such a model could help the oncologist to decide which best strategy should be undertaken (eg, starting an adjuvant therapy), in the case of chemotherapy. Consider some virtual patients with a breast cancer treated during 6 cycles of 21 days with a cocktail of Epirubicine (100mg) and Doxetaxel (75mg) as proposed in [46]. We use meanvalues of parameters for the drug as reported in [36], and represent a virtual patient by a set of parameters (a, θ, α, m). We fix the values of $a = 4.71 \times 10^{-4}$, $\theta = 10^{12}$, $\alpha = 2/3$ and let the value of m vary from $m = 1.7 \times 10^{-8}$ to $m = 6.1 \times 10^{-7}$. Table 2 shows that the last four patients present a highly metastatic risk five years after the end of the treatment. We suggest for the last four patients

Patients	m	# Metastases	Patients	m	# Metastases
$n°1$	1.7×10^{-8}	0	$n°6$	7.0×10^{-8}	0
$n°2$	1.9×10^{-8}	0	$n°7$	1.3×10^{-7}	**1**
$n°3$	2.7×10^{-8}	0	$n°8$	2.7×10^{-7}	**2**
$n°4$	5.0×10^{-8}	0	$n°9$	4.0×10^{-7}	**3**
$n°5$	6.1×10^{-8}	0	$n°10$	6.1×10^{-7}	**5**

Table 2: Metatstatic state of the patients, five years after the end of the treatment suggested in [46]

to increase the number of cycles of therapy or to use optimal protocol as described in the clinical essay MODEL I [35]. Table 3 shows adaptation of the number of cycles of the treatment or the use of an adapted therapy may reduce the metastatic risk for the patients.

Patients	m	Viens's protocol			Optimized protocol		
		6 cycles 126 days	9 cycles 189 days	12 cycles 252 days	9 cycles 126 days	13 cycles 182 days	18 cycles 252 days
$n°7$	1.3×10^{-7}	**1**	0	$\star$	0	$\star$	$\star$
$n°8$	2.7×10^{-7}	**2**	1	0	2	0	$\star$
$n°9$	4.0×10^{-7}	**3**	2	1	3	1	0
$n°10$	6.1×10^{-7}	**5**	4	3	4	3	1

Table 3: Metastatic state of the patients $n°7 - 10$ for various protocols

Identification of the parameter m would thus be crucial in view of clinical application. Our convinction is that the main information on metastatic aggressiveness lies in the primary tumor (as suggested in [17]) so that even if the patient is in a micro-metastatic state in an adjuvant setting we can hope to identify this parameter from histological data from the primary tumor.

https://doi.org/10.1051/mmnp/20127114 Published online by Cambridge University Press

3. Anti-angiogenic therapy

Another class of treatment consists in targeting the tumoral vasculature [21] since neo-angiogenesis is a fundamental process in cancer evolution, consisting for the tumor in developing its own vascular network. This process ensures nutrient's supply to the tumor and allows it to grow beyond 2-3 mm diameter. Anti-angiogenic (AA) therapies have emerged in the early 2000's as a new class of anticancer agents with limited toxicities. They are classified as small molecules (eg, tyrosine kinase inhibitors) and monoclonal antibodies. The rise of targeted therapies has generated a great hope in clinical oncology. However, despite marked achievements in increasing response rates, most of these new drugs failed in prolonging disease-free survival or overall survival in patients with cancer (see [24] for a synthesis of results of AA drugs). Determining the best temporal administration protocol for these agents is still a clinical open question [40, 24].

3.1. Model

In order to take into account for the effect of anti-angiogenic (AA) therapy, we consider the model of Hahnfeldt - Folkman [26] for vascular tumoral evolution, which has been biologically validated in [26] by comparison with mice data. It consists in taking the parameter θ from the Gompertz equation (2.1) as being related to the vasculature of the tumor and dynamically evolving in time, the dynamics resulting from the competition between endogenous stimulation and inhibition from the tumor in the following way

$$\dot{\theta}(t) = cx - dx^{2/3}\theta.$$

The two terms of this equation result from a ingenious analysis of the diffusion of inhibitory and stimulatory agents within the tumor which concludes to a constant rate of production for stimulating molecules and a rate of production proportional to the surface of the tumor for inhibitory ones, thus explaining the term in $x^{2/3}$. Anti-angiogenic therapy is then modeled by adding a log-kill term in this equation. Since we will consider situations with the combination of AA and CT, we also add a log-kill term in the Gompertz equation on the tumoral evolution. The growth rate is now two-dimensional and writes

$$G(t,X) = G(t,x,\theta) = \begin{pmatrix} ax\ln\left(\frac{\theta}{x}\right) - C(t)(x-x_{min})^+ \\ cx - dx^{2/3} - eA(t)(\theta-\theta_{min})^+ \end{pmatrix} \tag{3.1}$$

where $C(t)$ and $A(t)$ stand respectively for the CT and AA drug effective concentrations resulting from a PK/PD model and $x_{min} = \theta_{min}$ is the size of one cell, taken as minimal value for the drugs to be active.

We assume that the metastases have size x and vascular capacity θ (which has same unit than x) bigger than x_{min} and less than $b = \left(\frac{c}{d}\right)^{3/2}$ which is the maximal reachable size and vascular capacity by a tumor following the Hahnfeldt-Folkman model. Hence they evolve in the square $\Omega =]x_{min}, b[\times]x_{min}, b[$. The metastatic density is structured by a two-dimensional trait $X = (x,\theta)$ and solves the problem (1.1), with G given by (3.1). Considering that all metastases are born with size $x_{min} = 1$ cell = 10^{-6} mm^3 and vascular capacity θ_0 we take $N(\sigma) = \delta_{\sigma=(1,\theta_0)}$, the Dirac

https://doi.org/10.1051/mmnp/20127114 Published online by Cambridge University Press

mass at point $(1, \theta_0)$. We refer to [7, 8, 9] for mathematical and numerical analysis of the resulting two-dimensional, measure-valued renewal equation.

Mice parameters We use the parameters values obtained in [26] from fits to data on mice bearing Lewis Lung carcinoma. The metastatic parameters are fixed arbitrarily. The values are given in the Table 4.

a	c	d	θ_0	m	α
0.192	5.85	0.00873	625	0.001	2/3
day^{-1}	day^{-1}	$\text{day}^{-1}\text{mm}^{-2}$	mm^3	Nb of meta$\cdot\text{day}^{-1}\cdot$ $\text{mm}^{-3\alpha}$	

Table 4: Values of the growth and metastatic parameters for mice. Parameters a, c and d where fitted on mice data in [26].

Human parameters In the paper of Iwata et al. [28] where the growth rate was a Gompertz, parameters where identified from data on a hepatocellular carcinoma. To determine realistic parameters for human situations, we fix values of the parameters for the model of Hahnfeldt et al. reproducing the gompertzian growth curve of Iwata et al., keeping the carrying capacity from [28] equal to $\left(\frac{c}{d}\right)^{3/2}$ and fixing θ_0 as being rescaled from the value of [26] by the ratio of the maximal reachable sizes from the two papers. We use the same value for α and adapt the value of m to a size unit in mm^3 : in [28] $m = 5.3 \cdot 10^{-8}$(Number of metastases)$\cdot$(cell$^{-\alpha}$)$\cdot\text{day}^{-1}$ gives $m = 5.3 \cdot 10^{-8} \cdot 10^{6\alpha}\cdot$(Number of metastases)$\cdot(\text{mm}^{-3\alpha})\cdot\text{day}^{-1}$.

a	c	d	θ_0	m	α
0.0042	1	$5.7251\cdot 10^{-4}$	2630.14	$5.3\cdot 10^{-4}$	2/3
day^{-1}	day^{-1}	$\text{day}^{-1}\text{mm}^{-2}$	mm^3	Nb of meta$\cdot\text{day}^{-1}\cdot$ $\text{mm}^{-3\alpha}$	

Table 5: Values of the growth and metastatic parameters for human. a, m and α are from [28].

3.2. Results : Primary Tumor VS Metastases

We recall here various simulations of AA monotherapy that can be found in [8] and investigate the difference in effectiveness of various drugs regarding to their pharmacokinetic/pharmacodynamic parameters. The first result shown in Figure 1 takes the three drugs which were used in [26] where only the effect on tumor growth was investigated, and simulates the effect on the metastases. The three drugs are TNP-470, endostatin and angiostatin and each drug is characterized by two parameters in the model : its efficacy e and its clearance rate clr_A. The first one appears in the second

https://doi.org/10.1051/mmnp/20127114 Published online by Cambridge University Press

component of the growth rate (see expression 3.1) and the second one in the one-compartmental pharmacokinetics model for the concentration $A(t)$:

$$A(t) = D \sum_{i=1}^{N} e^{-clr(t-t_i)} \mathbf{1}_{t \geq t_i}, \tag{3.2}$$

where D is the administrated dose which is given as bolus at times t_i. These parameters were retrieved in [26] by fitting the model to mice data. The administration protocols are the same for endostatin and angiostatin (20 mg every day) but for TNP-470 the drug is administrated with a dose of 30 mg every two days.

We observe that TNP-470 seems to have the poorest efficacy, both on tumoral growth, vascular capacity and total number of metastases, due to its large clearance. As noticed in [26], the ratio e/clr_A should govern the efficacy of the drug and its value is 0.13 for TNP-470 and 0.39 for both endostatin and angiostatin. The model we developed is now able to simulate efficacy of the drugs on the metastatic evolution (figure 1.C). Interestingly, the drug which seems to be more efficient regarding to the tumor size at the end of the simulation (day 15), namely angiostatin, is not the one which gives the best result on the metastases. Indeed, the lower efficacy of endostatin regarding to ultimate size is due to a relatively high clearance provoking a quite fast rebound of the angiogenic capacity once the treatment stops. But since the tumor size was lower for longer time, the metastatic evolution was better contained. This shows that the model could be a helpful tool for the clinician since the response to a treatment can differ from the primary tumor to metastases, but the clinician has no data about micro-metastases which are not visible with imagery techniques.

In the figure 2, we investigate the influence of the AA dose (parameter D) on tumoral, vascular and metastatic evolution. We observe that the model is consistent since it exhibits a monotonous response to variation of the dose.

Influence of the scheduling One of our main postulate in the treatment of cancer is that for a given drug, the effect can vary regarding to the temporal administration protocol of the drug, due to the combination of the pharmacokinetic of the drug and the intrinsic dynamic of tumoral and metastatic growth. To investigate the effect of varying the administration schedule of the drug, we simulated various administration protocols for the same drug (endostatin). The results are presented in figure 3. We gave the same dose and the same number of administrations of the drug but either uniformly distributed during 10 days (endostatin 2), concentrated in 5 days (endostatin 1) or in 2 days and a half (endostatin 3).

We observe that the tumor growth is better stabilized with a uniform administration of the drug (endostatin 2) but the number of metastases is better reduced with the intermediate protocol (endostatin 1). It is interesting to notice that again if we look at the effects at the end of the simulation, the results are different for the tumor size and for the metastases. The two protocols endostatin 1 and endostatin 2 give the same size at the end, but not the same number of metastases. Moreover, the best protocol regarding to minimization of the final number of metastases (endostatin 1) is neither the one which provoked the largest regression of the tumor during the treatment (endostatin 3) nor the one with the most stable tumor dynamic (endostatin 2).

https://doi.org/10.1051/mmnp/20127114 Published online by Cambridge University Press

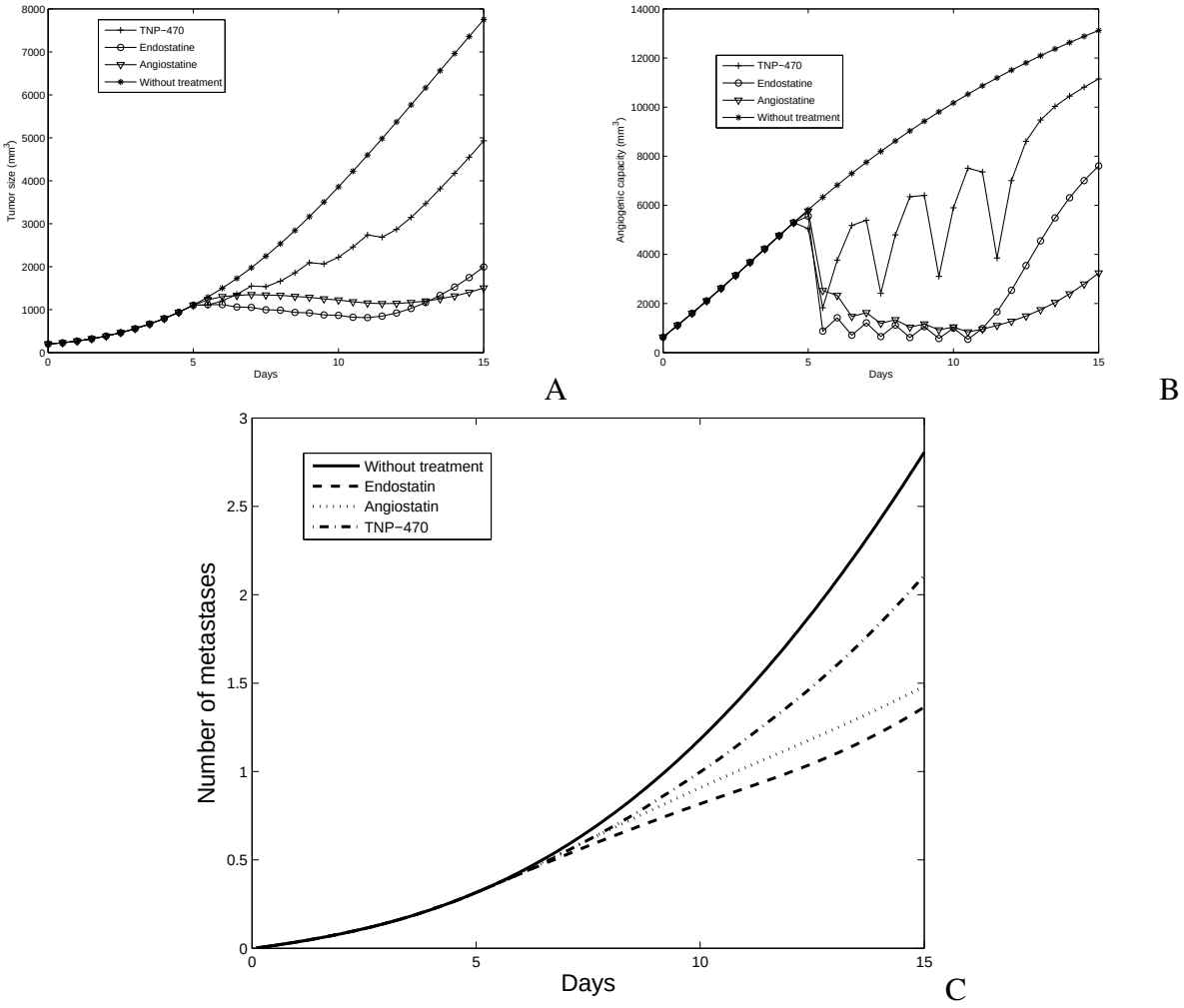


Figure 1: Effect of the three drugs from [26]. The treatment is administrated from days 5 to 10. Endostatin ($e = 0.66$, $clr_A = 1.7$) 20 mg every day, TNP-470 ($e = 1.3$, $clr_A = 10.1$) 30 mg every two days and Angiostatine ($e = 0.15$, $clr_A = 0.38$) 20 mg every day. A : tumor size. B : Angiogenic capacity. C : Number of metastases.

https://doi.org/10.1051/mmnp/20127114 Published online by Cambridge University Press

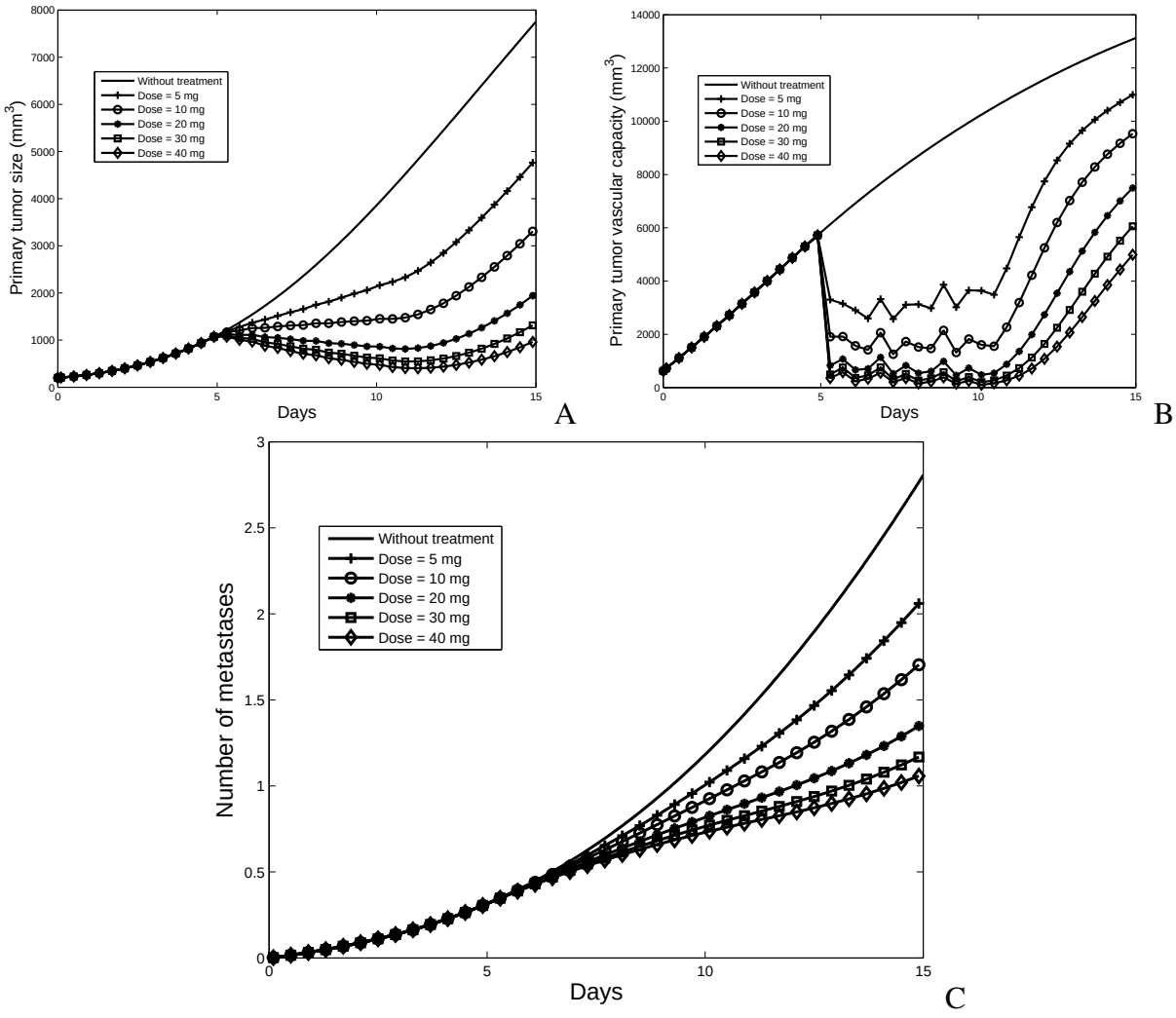


Figure 2: Effect of the variation of the dose for endostatin. A : tumor size. B : Angiogenic capacity. C : Number of metastases.

https://doi.org/10.1051/mmnp/20127114 Published online by Cambridge University Press

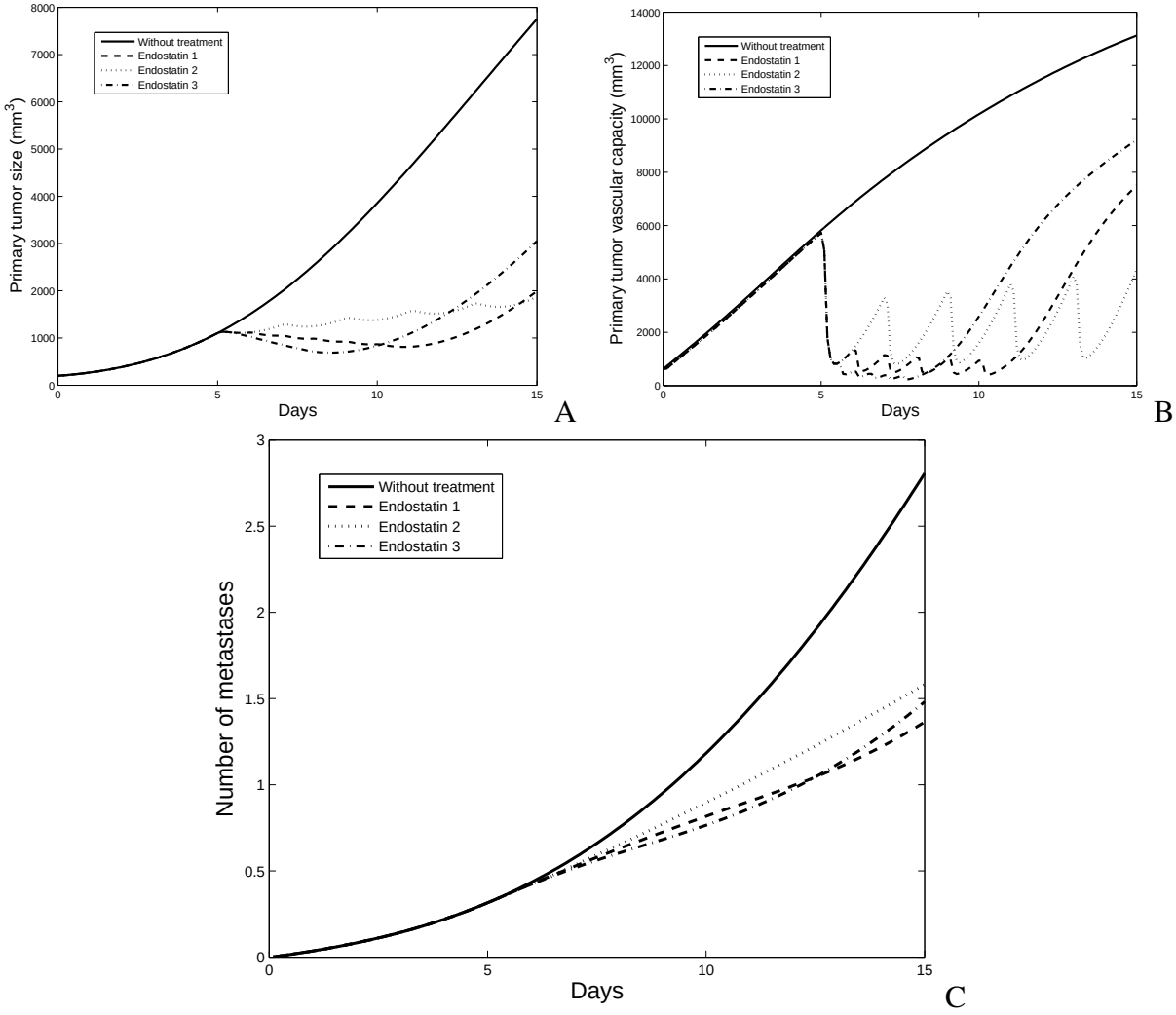


Figure 3: Three different temporal administration protocols for the same drug (Endostatin). Same dose (20 mg) and number of administrations (6) but more or less concentrated at the beginning of the treatment. Endostatin 1 : each day from day 5 to 10. Endostatin 2 : every two days from day 5 to 15. Endostatin 3 : twice a day from day 5 to 7.5. A : tumor size. B : Angiogenic capacity. C : Number of metastases.

https://doi.org/10.1051/mmnp/20127114 Published online by Cambridge University Press

3.3. Metastatic acceleration

In a recent paper [20], Ebos et al. obtained surprising results after AA therapy with Sunitinib, a tyrosine kinase inhibitor of VEGFR, a Vascular Endothelial Growth Factor (VEGF) receptor. The treatment could induce metastatic acceleration in mice, while substantially inhibiting primary tumor growth. They used two different experimental protocols to evidence this phenomenon, on mice : by intravenous injection of cancerous cells or by orthotopic implantation of a tumor in the mammary fat pad and then removal of the primary tumor. In both cases, they obtained acceleration of the metastatic mass in groups treated by the AA drug, compared to an untreated group. However, on the primary tumor, the effect of the treatment was beneficial, as shown in Figure 4A of [20]. Moreover, sustained therapy at 60 mg/kg/day exhibited better primary tumor slowdown than a temporal protocol of 120 mg/kg/day during 7 days, starting the day after tumor implantation. These results were corroborated by another paper by Paez-Ribes et al. [37] in the very same issue of the journal.

3.3.1. Model

In this subsection, we modify our model in order to qualitatively reproduce these results, in a first attempt to have a theoretical tool aiming at controlling this paradoxical metastatic acceleration effect. In [20], the authors propose as possible explanation for the phenomenon an upregulation of proangiogenic factors. To integrate this feature in the model, we propose to modify the angiogenesis stimulation parameter c of the tumoral growth model of Hahnfeldt - Folkman, only for the growth of metastases, by making it dependent of the AA drug concentration $A(t)$, with an increased value $c_M \gg c$ when the AA concentration is above a threshold A_τ :

$$c(A(t)) = \begin{cases} c_M & \text{if } A(t) \geq A_\tau \\ c & \text{if } A(t) < A_\tau \end{cases}$$

See Figure 4 for an illustration.

Our model is thus designed to take into account for the possible counter-attack of tumor cells towards AA therapy, as suggested by [20] and shown in [15]. Indeed, in this last paper the authors demonstrate an increase of VEGF tumoral expression after erlotinib therapy in an *in vitro* experiment.

The equation for the dynamics of the vasculature of the metastases during the therapy becomes

$$\frac{d\theta}{dt} = c(A(t))x - dx^{2/3}\theta - eA(t)(\theta - \theta_{min})^+ = G_2(t, x, \theta). \tag{3.3}$$

and we see that the effect of the treatment is balanced between this "boost" effect and the natural anti-angiogenic effect of the drug.

We justify the fact that this angiogenic boost effect only occurs on the metastases and not on the primary tumor in view of the following arguments :

1. The primary tumor is big and relatively stable concerning angiogenic dynamics, having already established a vascular network and thus it is less active regarding to this process. On

https://doi.org/10.1051/mmnp/20127114 Published online by Cambridge University Press

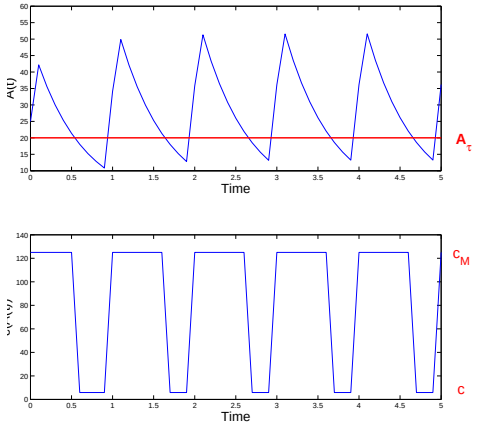


Figure 4: Illustration of activation of the boost effect.

the contrary, metastases are small and fully active, passing through the angiogenic switch. Hence they are more reactive to an external stress. We could be more accurate by making c_M depend on the size of the tumor. In first approximation though, we don't do so.

2. Metastases are known to be genetically more aggressive, as the detaching cells which give rise to a malignant secondary tumor must have survived to various adverse events (intravasation into blood vessels, extravasation, settling in a new environment...). Thus they could have a stronger reactive phenotype towards AA therapy.

In absence of pharmacokinetics data for the Sunitinib, we perform the simulations in the case of a one-compartmental PK model (equation (3.2)), with clearance equal to 1.7 (endostatin in [26]).

3.3.2. Simulations

Metastatic acceleration To perform the simulations, we use the tumoral growth parameters of Table 4. For the other parameters, we use

$$e = 0.2, \quad clr_A = 1.7, \quad c_M = 50, \quad m = 0.001, \quad \alpha = \frac{2}{3}, \quad (x_0, \theta_0) = (10^{-6}, 10^{-5}). \tag{3.4}$$

Of course, to obtain metastatic acceleration, we have to consider small value of the threshold A_τ, which can be approximated by taking $A_\tau = 0$ (immediate boost effect). In the Figure 5 are presented simulation results in this situation, which qualitatively reproduce the results of Figure 2A from [20]. We simulated the model without therapy, with initial primary tumor values $(x_{0,p}, \theta_{0,p}) = (1, 10^{-5})$, virtually performed resection of the primary tumor on day 14.5 (which consists in removing the source term in the PDE for the metastatic density) and then administrated the AA drug starting day 15, during 6 days. The temporal administration protocol that we used for the drug is 20mg/day. This result shows that for the parameter values (3.4), the model is able

https://doi.org/10.1051/mmnp/20127114 Published online by Cambridge University Press

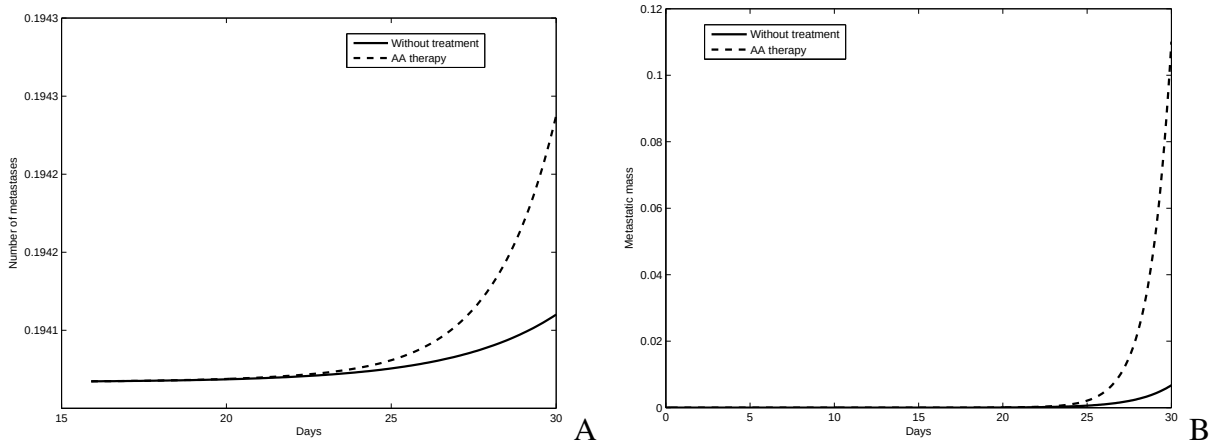


Figure 5: Metastatic acceleration for $A_\tau = 0$. A. Total number of metastases, only from day 15 to day 30. B. Metastatic mass

to reproduce metastatic acceleration, the balance between the anti-angiogenic effect and the boost effect in equation (3.3) being in favor of the second one.

In Figure 6, we reproduced *in silico* the situation of Figure 4A from [20] by not performing resection of the primary tumor and testing two different temporal protocols for the AA drug on primary tumor evolution : protocol 1 consists in giving the drug at 20mg/day during 7 days and protocol 2 administrates half of the dose, 10mg/day, but during a larger time, from day 13 (which is the time for which the tumor reaches 200mm^3 in the model) until the end. We also used $A_\tau = 0$ in this simulation. We observe good qualitative agreement between Figure 6.A, showing the primary tumor growth, and the Figure 4A from [20]. Indeed, since the primary tumor is not subjected to the boost effect in the model, the AA drug induces inhibition of the growth. We also retrieve the fact that better results are obtained with sustained therapy (protocol 2), on the primary tumor. In Figures 6.B, C and D we show some metastatic quantities, respectively the total number of metastases, the metastatic mass and the number of visible metastases (size exceeding 10^8 cells = 100 mm^3) . The following fact is interesting to notice : for both protocol, the total number of metastases is reduced compared to the situation without treatment; however, for the metastatic mass and the visible metastases, the effect depends on the protocol. While protocol 1 induces increased metastatic mass and number of visible metastases, protocol 2 has a positive effect, being even able to avoid apparition of visible metastases whereas protocol 1 provokes the presence of almost two visible metastases at the end of the simulation. It would be interesting to compare these *in silico* predictions to the metastatic data corresponding to Figure 4A from [20] (unfortunately not available in the paper).

We could imagine that the threshold value A_τ is a parameter which depends on the AA drug considered, or on the patient. Identification of its value would then be of fundamental importance since metastatic acceleration can occur or not depending on this value, as illustrated in Figure 7 where we performed the same numerical experiment as in Figure 5, but with $A_\tau = 20$, and observe

https://doi.org/10.1051/mmnp/20127114 Published online by Cambridge University Press

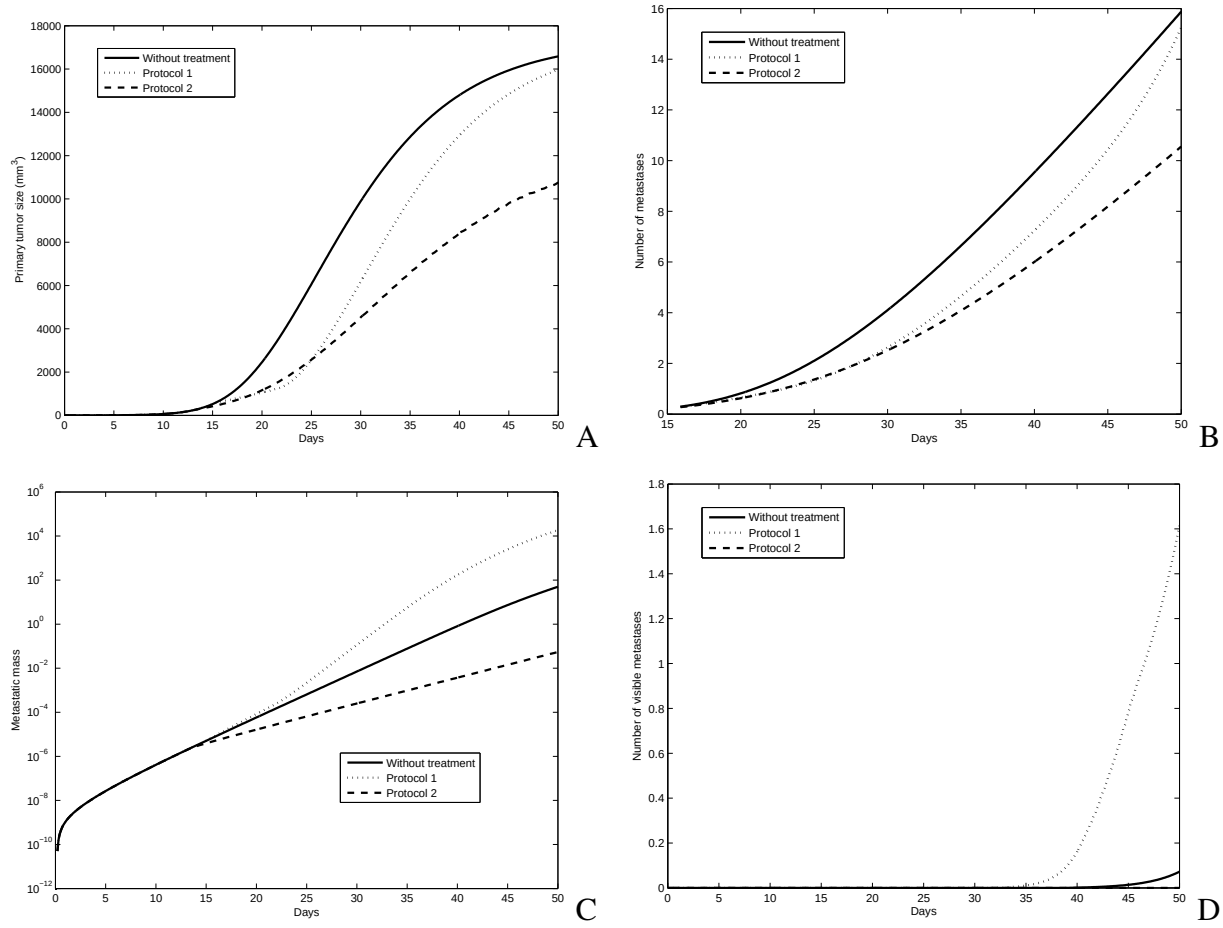


Figure 6: Without resection. Protocol 1 : 20mg/day from day 15 to day 21. 10mg/day from day 13 until the end A. Primary tumor. B. Total number of metastases, from day 15 until the end. C. Metastatic mass (log scale). D. Visible metastases

https://doi.org/10.1051/mmnp/20127114 Published online by Cambridge University Press

reduction of the total number of metastases and of the metastatic mass, that is, the opposite of Figure 5.

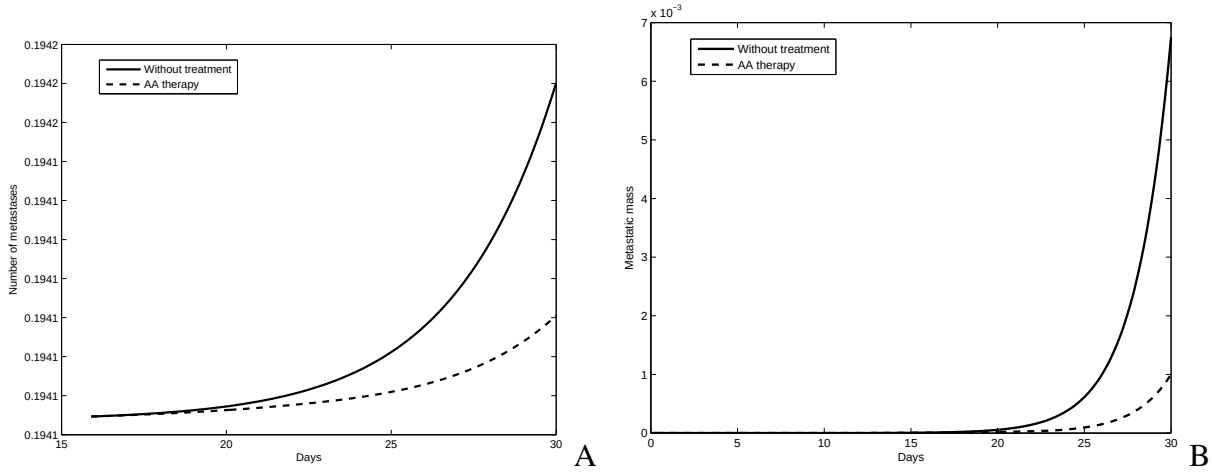


Figure 7: No metastatic acceleration for $A_\tau = 20$. A. Total number of metastases, only from day 15 to day 30. B. Metastatic mass

Influence of the scheduling In the Figure 8 we compare two protocols regarding to the metastatic acceleration phenomenon. Protocol 1 consists in giving the drug every day at dose 20 mg and Protocol 2 administrates the double dose every two days, each one being administrated from day 15 to 42 and with $A_\tau = 7$.

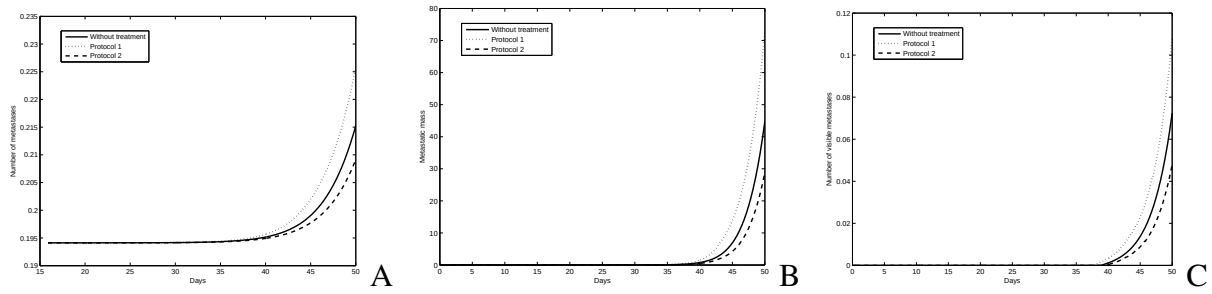


Figure 8: Influence of the scheduling. $A_\tau = 7$. Protocol 1 : 20 mg/day. Protocol 2 : 40 mg/2 days. A. Total number of metastases. B. Metastatic mass. C. Visible metastases

The two protocols have different implications : protocol 1 implies metastatic acceleration while protocol 2 results in deceleration of metastatic growth. These results are to be compared with the Figure 5 from the publication [19] concerning primary tumor evolution, where the equivalent protocols give the opposite qualitative results, namely a better effect of protocol 1. Of course, what we observe here in the metastatic acceleration context (i.e., using equation (3.3) for the vascular

https://doi.org/10.1051/mmnp/20127114 Published online by Cambridge University Press

dynamics of the metastases) is totally related to the PK of the drug. In comparing two schedulings, the one resulting in larger boost effect will be the one for which the total time above A_τ in the drug concentration time profile will be the largest (see Figure 4).

Again, the result depends on the value of the parameter A_τ, as shown in Figure 9 where we performed the same simulation with $A_\tau = 20$ and obtained the opposite result : protocol 1 is better than protocol 2.

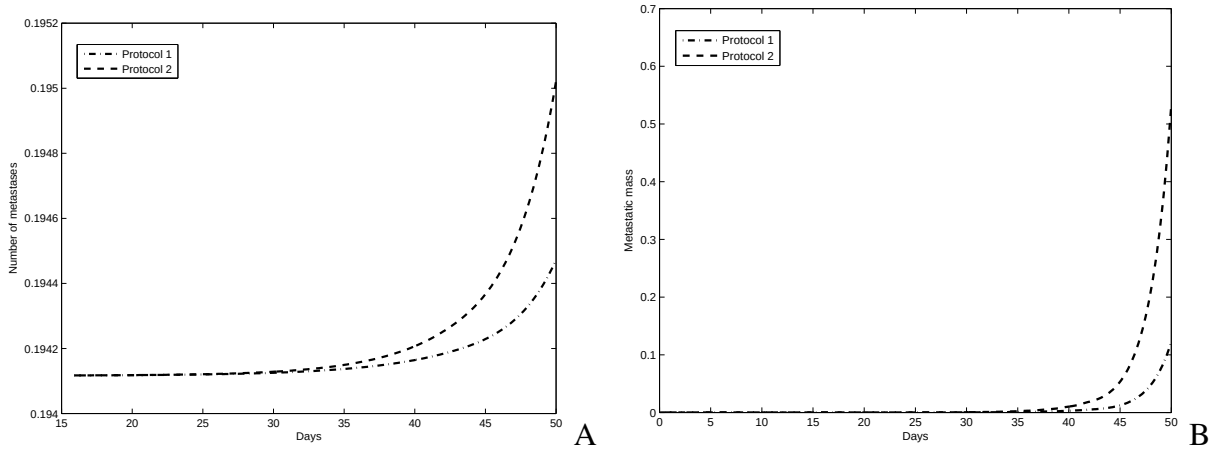


Figure 9: Influence of the scheduling. $A_\tau = 20$. Protocol 1 : 20 mg/day. Protocol 2 : 40 mg/2 days. A. Total number of metastases. B. Metastatic mass.

It would be interesting to perform biological experiments to identify the values of the threshold A_τ and of the overexpression of VEGF c_M. In particular they should probably depend on the drug under consideration. Estimating inter-individual variability of these parameters could reveal very helpful for designing better temporal administration protocols for AA agents.

4. Cytotoxic and anti-angiogenic drugs combination

Due to their poor anti-tumor efficacy, AA drugs are neither administered alone but rather in combination with classical chemotherapies. An important problem in clinical oncology is to determine how to combine a cytotoxic drug that kills the proliferative cells and an anti-angiogenic drug which acts on the angiogenic process. For instance, in [41], the authors obtained different response rates and overall survival depending on the scheduling of a CT composed of carboplatin and paclitaxel and erlotinib (tyrosin kinase inhibitor), in the case of non-small-cell lung cancer. Two questions are still open : which drug should come before the other and then what is the best temporal repartition for each drug? Here, we perform a brief *in silico* study of the first question.

The treatments impact by reducing the tumoral growth rate. Following the log-kill assumption for chemotherapy which says that cytotoxic drugs kill a constant fraction of the tumoral cells (and

https://doi.org/10.1051/mmnp/20127114 Published online by Cambridge University Press

not a constant number of them), the growth rate has the following expression

$$G(t,x,\theta) = \begin{pmatrix} ax\ln\left(\frac{\theta}{x}\right) - fC(t)(x-x_{min})^+ \\ cx - dx^{2/3} - eA(t)(\theta-\theta_{min})^+ \end{pmatrix}$$

and we will use the parameters from Table 5, except $m = 1$.

We place ourselves in the human case and consider combination of Etoposide,

Considering a clinical setting, we evaluate the combination between Etoposide, which is a CT agent used in wide variety of cancers (lung, testicle cancers, lymphoma, leukemia...) and Bevacizumab (monoclonal antibody targeting Vascular Endothelial Growth Factor, used mainly in colorectal and breast cancers). Several recent clinical trials have been evaluating the combination of both drugs in lung cancers and glioblastoma, with mixed results [42, 39, 30, 23]. The PK model and parameters for the CT drug are from [3] and for Bevacizumab from [34]. Both publications show that the PK of the two drugs can be described by a two-compartmental model :

$$\begin{cases} \frac{dc_1(t)}{dt} = -k_{12}c_1(t) + k_{21}c_2(t) + \frac{I(t)}{V} \\ \frac{dc_2(t)}{dt} = -k_{21}c_2(t) + k_{12}c_1(t). \end{cases}$$

and then $A(t)$, $C(t) = c_2(t)$ (for the respective parameters). The dose injection $I(t)$ can be expressed as in (2.3) with injection durations τ_C and τ_A and respective administration doses. The parameter values can be found in Tables 6 and 7. We take as non-zero initial condition the traits

Parameter	V_1	V_2	k_{10}	k_{20}	k_{12}	k_{21}	τ_A	e
Value	2.66	2.66	0.0779	0	0.223	0.215	90	0.01
Unit	L	L	day^{-1}	day^{-1}	day^{-1}	day^{-1}	min	$\text{L}\cdot\text{mg}^{-1}\cdot\text{day}^{-1}$

Table 6: Parameter values for the PK model for Bevacizumab. All parameters except e are from [34].

Parameter	V_1	V_2	k_{10}	k_{20}	k_{12}	k_{21}	τ_C	f
Value	25	15	1.6	9.36	0.4	0	24	25
Unit	L	L	day^{-1}	day^{-1}	day^{-1}	day^{-1}	h	$\text{L}\cdot\text{g}^{-1}\cdot\text{day}^{-1}$

Table 7: Parameter values for the PK model for Etoposide. All parameters except f are from [3].

$(x_{0,p}, \theta_{0,p}) = (17112, 44849)$ corresponding to the values reached by the primary tumor after 1000 days when starting with one cell and the parameters from Table 5, except $m = 1$. We also take the corresponding value of $\rho(1000)$ as ρ^0.

In the Figure 10 we compare each monotherapy case to the combined treatment with the two drugs. The administration protocol for Bevacizumab is 5 mg/kg/2 weeks [34] (with a virtual patient of 70 kg) and the Etoposide one is 0.5 g/m^2 at day 1 of the cycle [3] (virtual patient with a Body

https://doi.org/10.1051/mmnp/20127114 Published online by Cambridge University Press

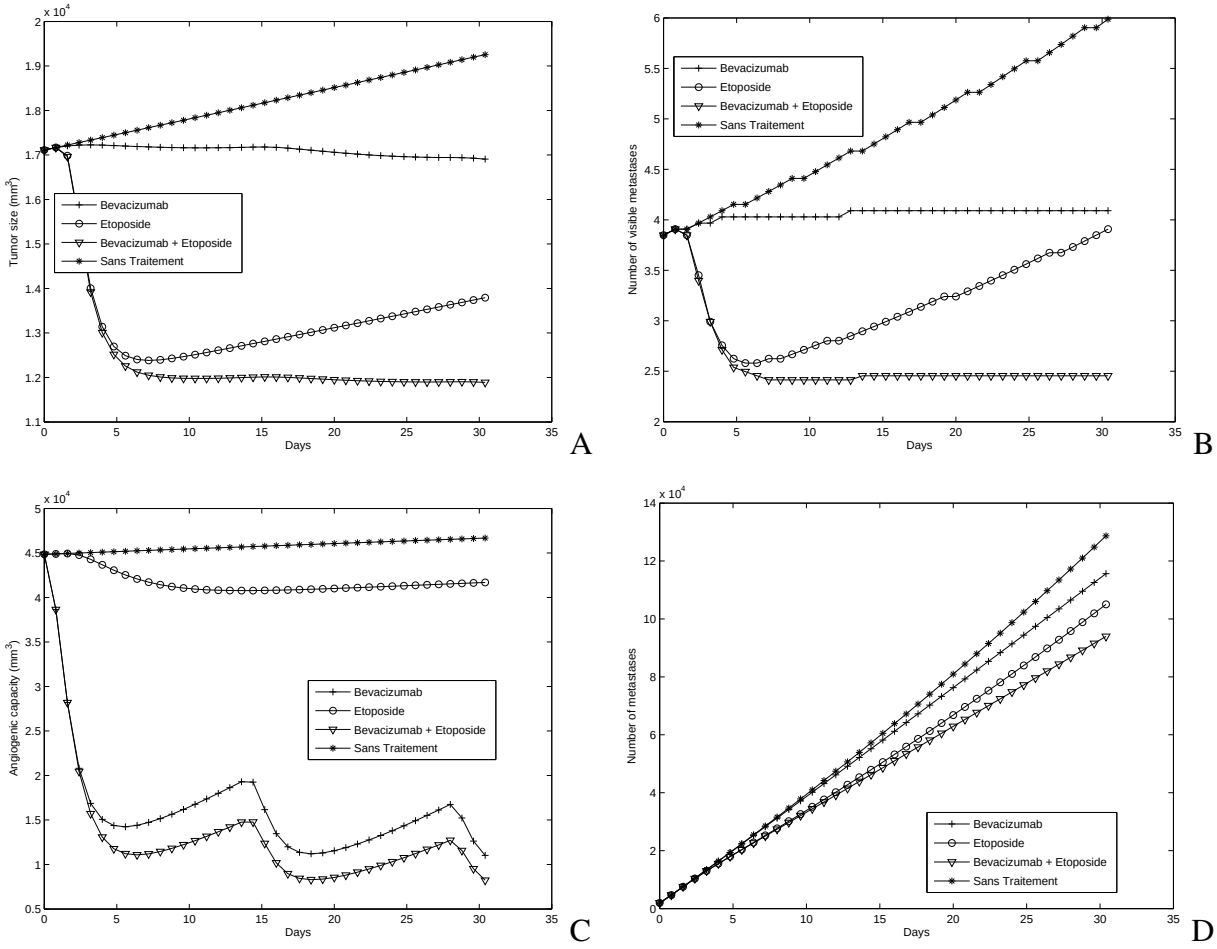


Figure 10: Comparison between the two monotherapy cases and the combined therapy. A : Primary tumor size. B : Visible metastases. C : Angiogenic capacity. D : Total number of metastases.

https://doi.org/10.1051/mmnp/20127114 Published online by Cambridge University Press

Surface Area of 1.75 m^2). We observe that, with the efficacy parameter e and f that we chose, the effect of the AA drug is to stabilize tumoral growth as well as the number of visible metastases. The CT has an important reduction effect and combination of both is better than the two monotherapy cases since it allows to reduce the tumor burden and then stabilize it to a low level.

We investigate now the effect of changing the order of administration of the two drugs. In the Figure 11 we simulated two situations with one administration of each drug : either Bevacizumab at day 0 and Etoposide at day 8 or the opposite.

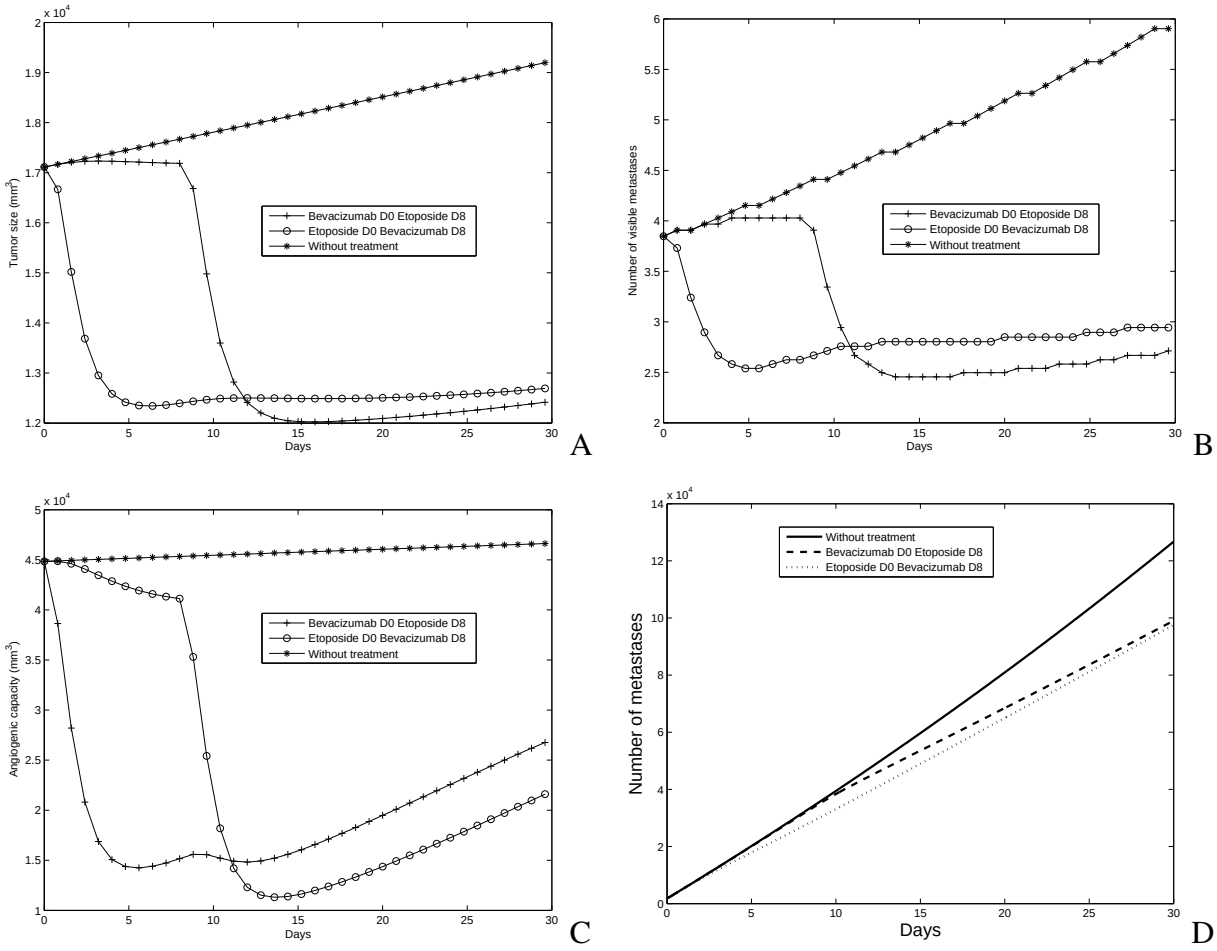


Figure 11: Administer the CT before or after the AA? A : Primary tumor size. B : Visible metastases. C : Angiogenic capacity. D : Total number of metastases.

An interesting fact to observe is that the best way of combining both regarding to the tumor size, namely AA first and then CT is not the best for the total number of metastases, which rather suggests that the best is the CT first and then the AA. Although the difference between both is very low we still have qualitatively different answers for primary tumor size and metastases, for the problem of the order of administration.

https://doi.org/10.1051/mmnp/20127114 Published online by Cambridge University Press

5. Metronomic chemotherapy

During the last decade, a novel therapeutic approach called *metronomic chemotherapy* (also named low dose anti-angiogenic therapy [12]) appeared. Various Phase I studies have been performed [1, 6, 14, 43, 16, 32, 44] using this new way of administrating cytotoxic agents which consists in giving the drug at low dose but as continuously as possible, whereas standard protocols administrate drugs at their respective MTD (maximal tolerated doses) as frequently as possible, with respect to the patient's hematological tolerance and the management of the drug-induced side effects. Indeed, this scheduling of the drug is believed to have better efficacy, one argument being that it would generate less resistances in the cancerous cells population in some circumstances. However, metronomic schedules are now thought to be potentially more efficient while reducing the toxicities according to the paradigm that this low dose/time dense scheduling of the drug would have important anti-angiogenic effect [31, 25]. Indeed, the endothelial cells which are proliferating during tumoral neo-angiogenesis are also targeted by the cytotoxic agent, while developping less resistances as they are genetically more stable than malignant cells. Moreover, the *dynamical* effect of metronomic schedules would be higher than the one of MTD protocols, for large times. In this context, determining what is the best metronomic scheduling for chemotherapeutic agents remains a major issue.

In this section, we use the Hahnfeldt - Folkman model to give insights on this topic, and observe the effect of metronomic schedules on the metastases population. As expressed above, one of the main ingredients explaining the benefit of metronomic schedules compared to MTD ones are the resistances, which we shall thus introduce in the model. We place ourselves in the context of breast cancer and will first consider a monotherapy situation with Docetaxel as the CT drug, and then combination of Docetaxel with Bevacizumab.

5.1. Model

The main assumptions underlying our modeling of the metronomic paradigm are the following :

1. The CT has an anti-angiogenic effect by killing proliferative endothelial cells.
2. Cancerous cells develop resistances to the CT whereas endothelial cells don't.
3. The killing action of the drug is stronger on the endothelial compartment than on the tumoral one (endothelial cells are more fragile).

We start from the Hahnfeldt - Folkman, in which we integrate anti-angiogenic effect of a chemotherapy (assumption 1). We consider that the CT drug acts in both compartment : on the tumoral compartment x (classical cytotoxic effect) and on the vasculature θ (anti-angiogenic effect due to the killing of proliferative endothelial cells). The expression of the growth rate G is

$$G(t,X) = \begin{pmatrix} ax\ln\left(\frac{\theta}{x}\right) - C_1(t)(x-x_{min})^+ \\ cx - dx^{2/3}\theta - (eA(t)+C_2(t))(\theta-\theta_{min})^+ \end{pmatrix} \tag{5.1}$$

https://doi.org/10.1051/mmnp/20127114 Published online by Cambridge University Press

where C_1 and C_2 are the exposures of the CT drug respectively on the tumoral cells and on the vascular compartment. They are defined from the output $C(t)$ of the PK model for Docetaxel (2.2), expressed in mg$\cdot$ L^{-1}. We take into account for the resistances (assumption 2) by assuming that for each time t, each cell has probability $RC(t)$ to become resistant. The probability of being resistant at time t is then exponentially distributed and we set

$$C_1(t) = \alpha_1 e^{-R\int_0^t C(s)ds} C(t), \quad C_2(t) = \alpha_2 C(t).$$

We transpose assumption 3 by taking $\alpha_2 > \alpha_1$. The parameter values are gathered in Tables 1 for the PK model and 8 for the PD one. For the metastatic evolution we use the model (1.1) with G

Parameter	α_I	β_I	α_1	α_2	R	τ
Value	0.75	25	0.5	5	5	60
Unit	day^{-1}	L·mg^{-1}	L·mg^{-1}·day^{-1}	L·mg^{-1}·day^{-1}	L·mg^{-1}·day^{-1}	min

Table 8: Parameter values for the PD model for Docetaxel. Values α_I and β_I come from [36]. Parameters α_1, α_2 and R were fixed arbitrarily.

being given by (5.1). The tumoral growth and metastatic parameters used in the simulations are those in Table 5 coming from [28] where they were fitted to data of a hepatocellular carcinoma. We take as non-zero initial condition the traits $(x_{0,p}, \theta_{0,p}) = (902.28, 15401)$ corresponding to the values reached by the primary tumor after 600 days when starting with one cell and the parameters from Table 5. We also take the corresponding value of $\rho(600)$ as initial metastatic density ρ^0.

5.2. Simulation results

Metronomic Docetaxel In the publication [6], for pediatric brain cancers, the authors compared a classical and a metronomic protocol. During 49-days therapy cycles, the classical protocol delivers 200 mg/m^2 of Temozolomide per day during the first 5 days whereas the metronomic protocol gives 85 mg/m^2 per day during 42 days followed by a 7-day rest period. The total amounts of drug delivered during a cycle are respectively 1000 mg/m^2 and 3570 mg/m^2, the second one being thus able to give more than 3.5 fold the total dose of the first one. We wish now to mimic this situation in the case of breast cancer with Docetaxel as CT and compare the two following schedules, based on a 21-day long therapy cycle :

1. MTD schedule : 100 mg at day 0, as considered in [36].
2. Metronomic schedule : 10 mg/day every day, without resting period.

The total dose administrated during one cycle are respectively 100 mg and 210 mg. The simulation results for the tumoral evolution and the metastases are presented in Figure 12.

We observe in Figure 12 that, at the beginning, the MTD schedule induces better tumoral reduction than the metronomic one, which exhibits only limited regression and even regrowth of

https://doi.org/10.1051/mmnp/20127114 Published online by Cambridge University Press

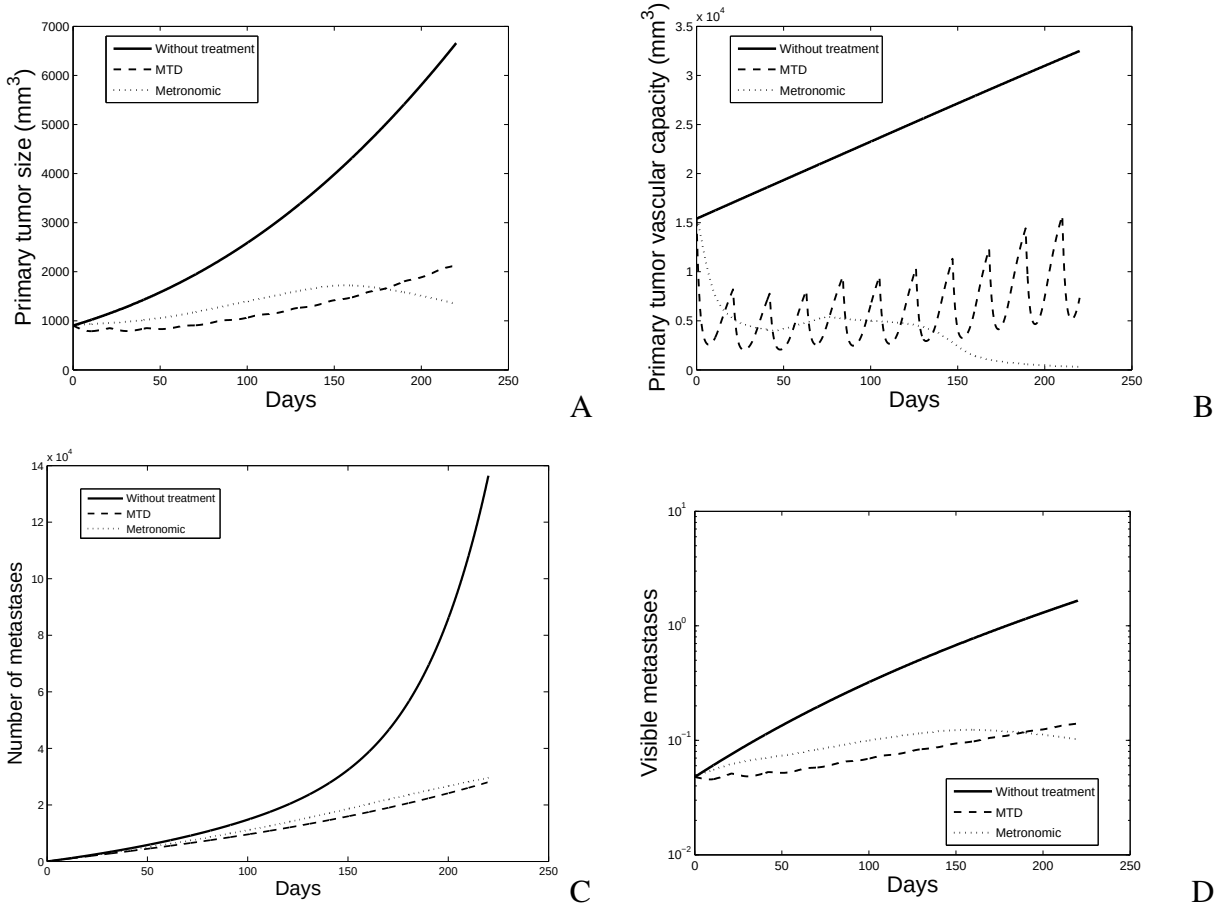


Figure 12: Comparison between MTD and metronomic schedules for Docetaxel. A. Primary tumor size. B. Primary tumor vascular capacity. C. Total number of metastases. D. Number of visible metastases (log scale).

https://doi.org/10.1051/mmnp/20127114 Published online by Cambridge University Press

the tumor. This could be misleading in practical situations since one could decide to stop the therapy when observing the regrowth. However, due to resistances the MTD schedule gets worse and eventually doesn't contain regrowth of the primary tumor. On the opposite, over long periods the metronomic schedule gives better results, being able to overcome the resistance phenomenon, and eventually leading to stable tumoral reduction, which still persists for times bigger than 220 days (simulation not shown). The explanation of this fact can be understood by looking at Figure 12.B representing the effect of the drug on the vascular capacity. While the MTD schedule does not provoke overall decrease of the vascular capacity on large time scale, the metronomic one ensures deeper and more stable effect on the vasculature, which eventually explains the large time tumor decrease. Hence, the overall superiority of the metronomic schedule is explained in the model by the anti-angiogenic action of the drug. The MTD schedule does also exhibit anti-angiogenic effect but, combined with the intrinsic dynamic of the vasculature, it is not asymptotically efficient because the large rest period lets time for the vasculature to recover. The metronomic schedule on the opposite does not let time for vascular recovery and, since endothelial cells are not subjected to resistances to the drug, is more efficient on large time scale.

Concerning metastases, we observe the same behavior as described above on the number of visible metastases (Figure 12.D). While the untreated curve leads to apparition of one visible metastasis at the end of the simulation, both protocols don't. But the MTD schedule asymptotically has growing number of visible tumors whereas the metronomic one is able to decrease it and keep it under control. On the total number of metastases, the MTD schedule is slightly better but we can suspect that for larger times both curves will cross since, according to Figure 12.A, all tumors will eventually decrease, thus leading to less emission of neo-metastases.

If the dose used in the metronomic schedule is too low, then it is not efficient, as shown in Figure 13 where the same metronomic schedule is simulated, but using a dose of 8 mg/day.

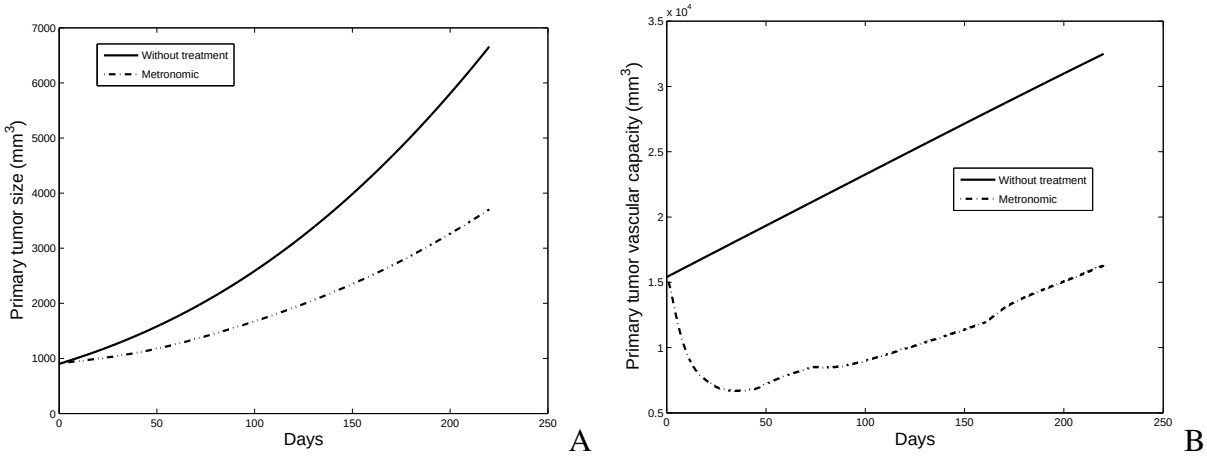


Figure 13: Metronomic schedule for Docetaxel with dose 8 mg/day. A. Tumor size. B. Vascular capacity

https://doi.org/10.1051/mmnp/20127114 Published online by Cambridge University Press

This result suggests that there is an optimal dose to use for metronomic schedules, and a mathematical model can be helpful in determining this optimum (see [10] for an optimal control problem for the scheduling). Integrating the toxicity issue in the model should help to further optimize the optimization of metronomic scheduling.

Metronomic Docetaxel + Bevacizumab We perform now the same comparison between the metronomic schedule and the classical one, but we add action of Bevacizumab. The scheduling that we use for this last drug comes from [34] and is 7.5 mg/kg every three weeks (Bevacizumab has a large half-life). We consider a virtual patient of 70 kg. The simulation results are plotted in Figure 14.

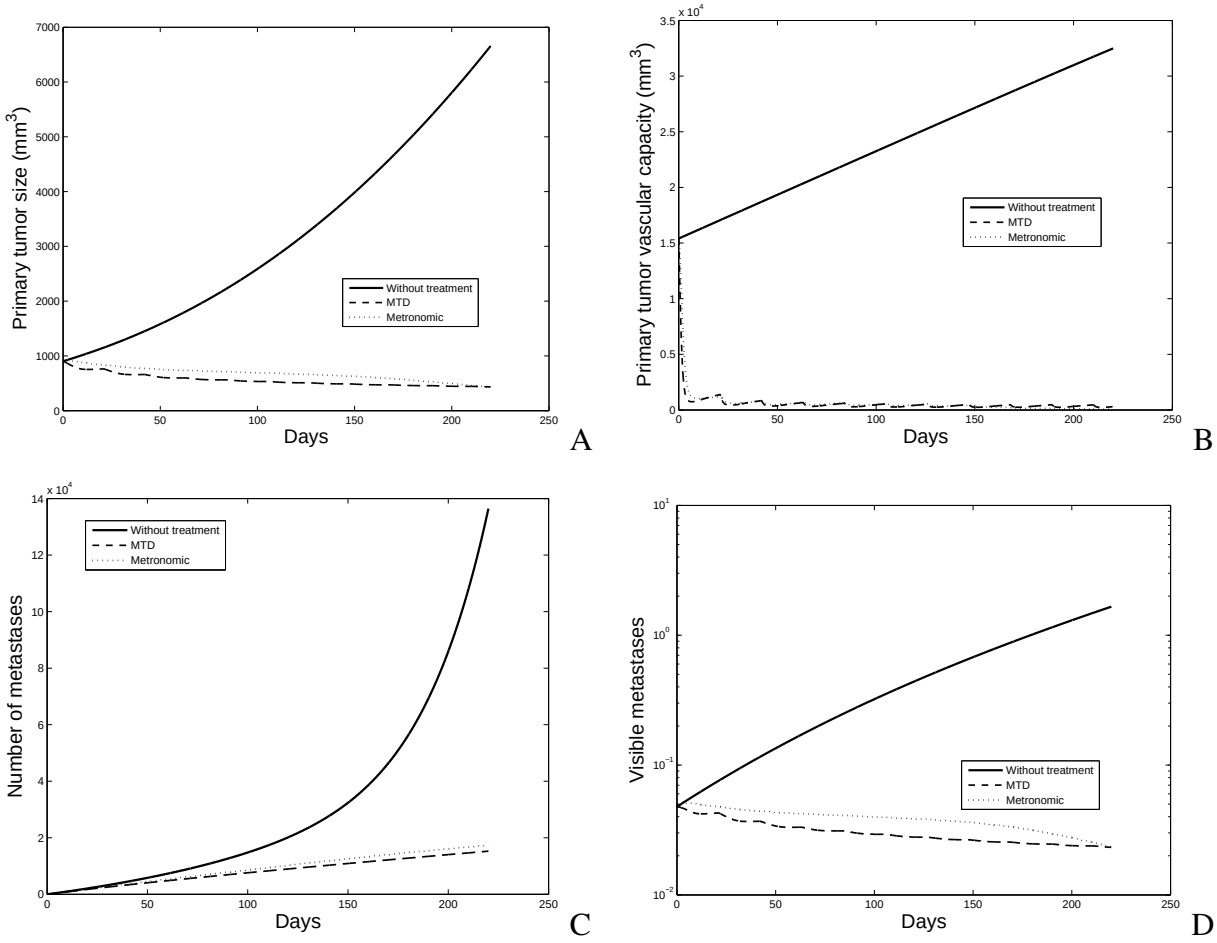


Figure 14: Comparison between MTD and metronomic schedules for Docetaxel in combination with Bevacizumab. A. Primary tumor size. B. Primary tumor vascular capacity. C. Total number of metastases D. Number of visible metastases (log scale).

We observe that the two scheduling efficiently reduce the tumor size and control explosion

https://doi.org/10.1051/mmnp/20127114 Published online by Cambridge University Press

of the total number of metastases and of the visible ones. If we look at evolution during the whole simulation, the classical schedule is better than the metronomic one. Indeed, as shown in Figure 14.B when comparing it with Figure 12.B, addition of the AA drug ensures large reduction of the vasculature leading to tumor suffocation. This happens independently from the temporal administration protocol of the CT drug. Our model suggests thus no benefit of the metronomic schedule on the classical one in the case of combination therapy with AA drugs.

6. Conclusion

One of the main issue in cancer therapy is to evaluate the metastatic risk of the patient. Determining the best regimen and the optimal dosing schedule is still an unsolved question in various clinical settings. Oncogenetics, pharmacogenomics and pharmacogenetics are new tools increasingly used that are dedicated to provide biomarkers for treatment efficacy and tolerance. Similarly, mathematical modeling could help and give valuable information to the physician to optimize treatments. The models that we presented in this paper can give informations on the (micro)metastatic state of the patient and the impact of therapy on its evolution. They deliberately involve a few number of parameters in view of clinical applications. We illustrated through numerical simulations how our models could be used to give insights on concrete clinical issues.

The models are flexible enough to integrate action of the two main chemical therapies available to clinicians : cyototoxic and anti-angiogenic. We were able to qualitatively reproduce experimental observations such as metastatic acceleration after AA therapy and to test biological hypotheses susceptible to provide rationale for the use of metronomic schedules in chemotherapy. The models were then used to run predictive *in silico* tests which have now to be confronted to biological data. We are currently performing mice experiments to validate the model in the ANR project MEMOREX-PK.

All along the study, we tried to use as much as possible parameter values coming from biological data available in the literature. However, all parameters were not available, in particular for metastatic emission and efficacy of the drugs. A possible way to estimate these last ones is to use results of clinical studies giving various evolution percentages of the disease (Complete Remission, Partial Remission, Stable Disease, Progressive Disease). The parameters can be calibrated using statistical methods to reproduce these results, as done for example in [5]. About the metastatic emission parameters m and α, we are currently working on methods to identify them from data on the primary tumor.

We are aware that, since our ultimate goal is to provide effective results in the clinic, it is mandatory to take into account for the toxicities induced by the considered therapies (hematological toxicities, mucositis, cutaneous rushes,...). Models dealing with these issues like [35, 4, 27] could be integrated in future versions. Furthermore, in the model we presented for combination of CT and AA therapies no nonlinear interactions between the drugs are taken into account. But since delivery of the CT depends on the amount of blood vessels reaching the tumor, a negative effect of AA therapy on the CT could be expected. On the opposite, a "normalization" effect [29] could also temporarily happen following administration of AA agents, thus improving CT transportation. We

https://doi.org/10.1051/mmnp/20127114 Published online by Cambridge University Press

are currently working on a refinement of the Hahnfeldt - Folkman model which deals with these features (See [11]).

The actual therapies are still experiencing various problems. This work shows that mathematical modeling could help to provide new leads to overcome the failures faced up to now.

Acknowlegments

The authors were partially supported by l'Agence Nationale de la Recherche under grant ANR-09-BLAN-0217-01 and a Grant # 50009 from the Association pour la Recherche contre le Cancer (ARC).

References

[1] N. André, A. Rome, C. Coze, L. Padovani, E. Pasquier, L. Camoin, and J.-C. Gentet. *Metronomic etoposide/cyclophosphamide/celecoxib regimen to children and adolescents with refractory cancer : a preliminary monocentric study*. Clin. Therapeutics, 30 (2008), No. 7, 1336–1340.

[2] D. Barbolosi, A. Benabdallah, F. Hubert, and F. Verga. *Mathematical and numerical analysis for a model of growing metastatic tumors*. Math. Biosci., 218 (2009), No. 1, 1–14.

[3] D. Barbolosi, G. Freyer, J. Ciccolini, and A. Iliadis. *Optimisation de la posologie et des modalités d'administration des agents cytotoxiques à l'aide d'un modèle mathématique*. Bulletin du Cancer, 90 (2003), No. 2, 167–175.

[4] D. Barbolosi and A. Iliadis. *Optimizing drug regimens in cancer chemotherapy: a simulation study using a pk–pd model*. Comput. Biol. Med., 31 (2001), 157–172.

[5] D. Barbolosi, F. Verga, A. Benabdallah, F. Hubert, C. Mercier, J. Ciccolini, and C. Faivre. *Modélisation du rique d'évolution métastatique chez les patients supposés avoir une maladie localisée*. Oncologie, 13 (2011), No. 8, 528–533.

[6] S. Baruchel, M. Diezi, D. Hargrave, D. Stempak, J. Gammon, A. Moghrabi, MJ. Coppes, C.V. Fernandez, and E. Bouffet. *Safety and pharmacokinetics of temozolomide using a dose-escalation, metronomic schedule in recurrent paediatric brain tumours*. Eur. J. Cancer, 42 (2006), 2335–2342.

[7] S. Benzekry. *Mathematical analysis of a two-dimensional population model of metastatic growth including angiogenesis*. J. Evol. Equ., 11 (2011), No. 1, 187.

[8] S. Benzekry. *Mathematical and numerical analysis of a model for anti-angiogenic therapy in metastatic cancers*. M2AN, 46 (2012), No. 2, 207–237.

https://doi.org/10.1051/mmnp/20127114 Published online by Cambridge University Press

[9] S. Benzekry. *Passing to the limit 2D-1D in a model for metastatic growth*. To appear in J. Biol. Dyn., (2011), http://hal.archives-ouvertes.fr/hal-00521968/fr/.

[10] S. Benzekry and A. Benabdallah. *An optimal control problem for anti-cancer therapies in a model for metastatic evolution*. In preparation (2011), http://hal.archives-ouvertes.fr/hal-00521968/fr/.

[11] S. Benzekry, G. Chapuisat, J. Ciccolini, A. Erlinger, and Hubert F., *A new mathematical model for optimizing the combination between anti-angiogenic and cytotoxic drugs in oncology*. In preparation (2011), http://hal.archives-ouvertes.fr/hal-00641476/fr/.

[12] T. Browder, C. E. Butterfield, B. M. Kraling, B. Shi, B. Marshall, M. S. O'Reilly, and J. Folkman. *Antiangiogenic scheduling of chemotherapy improves efficacy against experimental drug-resistant cancer*. Cancer Res., 60 (2000), 1878–1886.

[13] R. Bruno, N. Vivier, J. C. Vergniol, S. L. De Phillips, G. Montay, and L. B. Sheiner. *A population pharmacokinetic model for docetaxel (Taxotere): model building and validation*. J. Pharmacokinet Biopharm., 24 (1996), 153–172.

[14] M. Casanova, A. Ferrari, G. Bisogno, J. H. Merks, G. L. De Salvo, C. Meazza, K. Tettoni, M. Provenzi, I. Mazzarino, and M. Carli. *Vinorelbine and low-dose cyclophosphamide in the treatment of pediatric sarcomas: pilot study for the upcoming European Rhabdomyosarcoma Protocol*. Cancer, 101 (2004), 1664–1671.

[15] M. Chefrour, J. L. Fischel, P. Formento, S. Giacometti, R. M. Ferri-Dessens, H. Marouani, M. Francoual, N. Renee, C. Mercier, G. Milano, and J. Ciccolini. *Erlotinib in combination with capecitabine (5'dFUR) in resistant pancreatic cancer cell lines*. J. Chemother., 22 (2010), 129–133.

[16] L. M. Choi, B. Rood, N. Kamani, D. La Fond, R. J. Packer, M. R. Santi, and T. J. Macdonald. *Feasibility of metronomic maintenance chemotherapy following high-dose chemotherapy for malignant central nervous system tumors*. Pediatr. Blood Cancer, 50 (2008), 970–975.

[17] E. Comen, L. Norton, and J. Massague. *Clinical implications of cancer self-seeding*. Nat. Rev. Clin. Oncol., 8 (2011), 369–377.

[18] A. Devys, T. Goudon, and P. Laffitte. *A model describing the growth and the size distribution of multiple metastatic tumors*. Discret. and contin. dyn. syst. series B, 12 (2009), No. 4.

[19] A. d'Onofrio, A. Gandolfi, and A. Rocca. *The dynamics of tumour-vasculature interaction suggests low-dose, time-dense anti-angiogenic schedulings*. Cell Prolif., 42 (2009), 317–329.

[20] J. M.L. Ebos, C. R. Lee, W. Crus-Munoz, G. A. Bjarnason, and J. G. Christensen. *Accelerated metastasis after short-term treatment with a potent inhibitor of tumor angiogenesis*. Cancer Cell, 15 (2009), 232–239.

https://doi.org/10.1051/mmnp/20127114 Published online by Cambridge University Press

[21] J. Folkman. *Antiangiogenesis : new concept for therapy of solid tumors*, Ann. Surg., 175 (1972), 409–416.

[22] A. Fontana, A. Falcone, L. Derosa, T. Di Desidero, R. Danesi, and G. Bocci. *Metronomic chemotherapy for metastatic prostate cancer: a 'young' concept for old patients?*. Drugs Aging, 27 (2010), 689–696.

[23] A. B. Francesconi, S. Dupre, M. Matos, D. Martin, B. G. Hughes, D. K. Wyld, and J. D. Lickliter. *Carboplatin and etoposide combined with bevacizumab for the treatment of recurrent glioblastoma multiforme*. J. Clin. Neurosci., 17 (2010), 970–974.

[24] G. Gasparini, R. Longo, M. Fanelli, and B. A. Teicher. *Combination of antiangiogenic therapy with other anticancer therapies: Results, challenges, and open questions*. Journal of Clinical Oncology, 23 (2005), No. 6 1295–1311.

[25] P. Hahnfeldt, J. Folkman, and L. Hlatky. *Minimizing long-term tumor burden : the logic for metronomic chemotherapeutic dosing and its antiangiogenic basis*. J. Theor. Biol., 220 (2003), 545–554.

[26] P. Hahnfeldt, D. Panigraphy, J. Folkman, and L. Hlatky. *Tumor development under angiogenic signaling : a dynamical theory of tumor growth, treatment, response and postvascular dormancy*. Cancer Research, 59 (1999), 4770–4775.

[27] A. Iliadis and D. Barbolosi. *Optimizing drug regimens in cancer chemotherapy by an efficacy-toxicity mathematical model*. Comput. Biomed. Res., 33 (2000), 211–226.

[28] K. Iwata, K. Kawasaki, and Shigesada N. *A dynamical model for the growth and size distribution of multiple metastatic tumors*. J. Theor. Biol., 203 (2000), 177–186.

[29] R. K. Jain. *Normalizing tumor vasculature with anti-angiogenic therapy: A new paradigm for combination therapy*. Nature Medicine, 7 (2001), 987–989.

[30] K. Jordan, H. H. Wolf, W. Voigt, T. Kegel, L. P. Mueller, T. Behlendorf, C. Sippel, D. Arnold, and H. J. Schmoll. *Bevacizumab in combination with sequential high-dose chemotherapy in solid cancer, a feasibility study*. Bone Marrow Transplant., 45 (2010), 1704–1709.

[31] R.S. Kerbel and B.A. Kamen. *The anti-angiogenic basis of metronomic chemotherapy*. Nature Reviews Cancer, 4 (2004), 423–436.

[32] M. W. Kieran, C. D. Turner, J. B. Rubin, S.N. Chi, M.A. Zimmerman, C. Chordas, G. Klement, A. Laforme, A. Gordon, A. Thomas, D. Neuber, T. Browder, and J. Folkman. *A feasibility trial of antiangiogenic (metronomic) chemotherapy in pediatric patients with recurrent or progressive cancer*. J. Pediatr. Hematol. Oncol., 27 (2005), No. 11, 573–581.

[33] S. Koscielny, M. Tubiana, M. G. Le, A. J. Valleron, H. Mouriesse, G. Contesso, and D. Sarrazin. *Breast cancer: relationship between the size of the primary tumour and the probability of metastatic dissemination*. Br. J. Cancer, 49 (1984), 709–715.

https://doi.org/10.1051/mmnp/20127114 Published online by Cambridge University Press

[34] J. F. Lu, R. Bruno, S. Eppler, W. Novotny, B. Lum, and J. Gaudreault. *Clinical pharmacokinetics of bevacizumab in patients with solid tumors*. Cancer Chemother. Pharmacol., 62 (2008), 779–786.

[35] C. Meille, J. C. Gentet, D. Barbolosi, N. Andre, F. Doz, and A. Iliadis. *New adaptive method for phase I trials in oncology*. Clin. Pharmacol. Ther., 83 (2008), 873–881.

[36] C. Meille, A. Iliadis, D. Barbolosi, N. Frances, and G. Freyer. *An interface model for dosage adjustment connects hematotoxicity to pharmacokinetics*. J. Pharmacokinet. Pharmacodyn., 35 (2008), 619–633.

[37] M. Paez-Ribes, E. Allen, J. Hudock, T. Takeda, H. Okuyama, F. Vinals, M. Inoue, G. Bergers, D. Hanahan, and O. Casanovas. *Antiangiogenic therapy elicits malignant progression of tumors to increased local invasion and distant metastasis*. Cancer Cell, 15 (2009), 220–231.

[38] E. Pasquier, M. Kavallaris, and N. Andre. *Metronomic chemotherapy: new rationale for new directions*. Nat. Rev. Clin. Oncol., 7 (2010), 455–465.

[39] D. A. Reardon, A. Desjardins, K. Peters, S. Gururangan, J. Sampson, J. N. Rich, R. McLendon, J. E. Herndon, J. Marcello, S. Threatt, A. H. Friedman, J. J. Vredenburgh, and H. S. Friedman. *Phase II study of metronomic chemotherapy with bevacizumab for recurrent glioblastoma after progression on bevacizumab therapy*. J. Neurooncol., 103 (2011), 371–379.

[40] A. R. Reynolds. *Potential relevance of bell-shaped and u-shaped dose-responses for the therapeutic targeting of angiogenesis in cancer*. Dose-Response, 8 (2010), 253–284.

[41] G. J. Riely, N. A. Rizvi, M. G. Kris, D. T. Milton, D. B. Solit, N. Rosen, E. Senturk, C. G. Azzoli, J. R. Brahmer, F. M. Sirotnak, V. E. Seshan, M. Fogle, M. Ginsberg, Miller V. A., and C. M. Rudin. *Randomized phase ii study of pulse erlotinib before or after carboplatin and paclitaxel in current or former smokers with advanced non-small-cell lung cancer*. J. Clin. Oncol., 27 (2009), No. 2, 264–270.

[42] D. R. Spigel, P. M. Townley, D. M. Waterhouse, L. Fang, I. Adiguzel, J. E. Huang, D. A. Karlin, L. Faoro, F. A. Scappaticci, and M. A. Socinski. *Randomized Phase II Study of Bevacizumab in Combination With Chemotherapy in Previously Untreated Extensive-Stage Small-Cell Lung Cancer: Results From the SALUTE Trial*. J. Clin. Oncol., 29 (2011), 2215–2222.

[43] D. Stempak, J. Gammon, J. Halton, A. Moghrabi, G. Koren, and S. Baruchel. *A pilot pharmacokinetic and antiangiogenic biomarker study of celecoxib and low-dose metronomic vinblastine or cyclophosphamide in pediatric recurrent solid tumors*. J. Pediatr. Hematol. Oncol., 28 (2006), 720–728.

[44] J. Sterba, D. Valik, P. Mudry, T. Kepak, Z. Pavelka, V. Bajciova, K. Zitterbart, V. Kadlecova, and P. Mazanek. *Combined biodifferentiating and antiangiogenic oral metronomic therapy is*

https://doi.org/10.1051/mmnp/20127114 Published online by Cambridge University Press

feasible and effective in relapsed solid tumors in children: single-center pilot study. Onkologie, 29 (2006), 308–313.

[45] F. Verga. *Modélisation mathématique de processus métastatiques*. Ph.D. thesis, Université de Provence, 2010.

[46] P. Viens, H. Roche, P. Kerbrat, P. Fumoleau, J. P. Guastalla, and T. Delozier. *Epirubicin–docetaxel combination in first-line chemotherapy for patients with metastatic breast cancer: final results of a dose-finding and efficacy study*. Am. J. Clin. Oncol., 24 (2001), 328–335.

https://doi.org/10.1051/mmnp/20127114 Published online by Cambridge University Press